

# Comparing Rotary Bend Wire Fatigue Test Methods at Different Test Speeds

Jason D. Weaver and Erick J. Gutierrez

(Submitted October 13, 2015; published online October 30, 2015)

Given its relatively simple setup and ability to produce results quickly, rotary bend fatigue testing is becoming commonplace in the medical device industry and is the subject of a new standard test method ASTM E2948-14. Although some research has been conducted to determine if results differ for different rotary bend fatigue test setups or test speeds, these parameters have not been extensively studied together. In this work, we investigate the effects of these two parameters on the fatigue life of three commonly used medical device alloys (ASTM F2063 nitinol, ASTM F138 stainless steel, and ASTM F1058 cobalt chromium). Results with three different rotary bend fatigue test setups revealed no difference in fatigue life among those setups. Increasing test speed, however, between 100 and 35,000 RPM led to an increased fatigue life for all three alloys studied (average number of cycles to fracture increased between 2.0 and 5.1 times between slowest and fastest test speed). Supplemental uniaxial tension tests of stainless steel wire at varying strain rates showed a strain rate dependence in the mechanical response which could in part explain the increased fatigue life at faster test speeds. How exactly strain rate dependence might affect the fatigue properties of different alloys at different alternating strain values requires further study. Given the difference in loading rates between benchtop fatigue tests and in vivo deformations, the potential for strain rate dependence should be considered when designing durability tests for medical devices and in extrapolating results of those tests to in vivo performance.

**Keywords** biomaterial, test speed, wire fatigue

## 1. Introduction

Wires that are subjected to cyclic loading are used in a large number of medical devices in the dental, orthopedic, and cardiovascular fields (Ref 1-5). One of the most common ways to determine the fatigue properties of small diameter wires is through rotary bend fatigue testing. Rotary bend wire fatigue is a versatile test that can be used to compare fatigue properties of wires with a wide range of different characteristics including processing method, composition, and diameter (Ref 6-10). For biomedical applications, testing is typically conducted in deionized water or phosphate-buffered saline (PBS) at 37 °C to mimic the in vivo environment. Testing is conducted by taking a straight segment of wire, constraining it into a curved shape, gripping one or both wire ends, and then spinning the wire so that it undergoes alternating tensile and compressive stresses. Tests are typically conducted in either an unguided or guided fashion as shown in Fig. 1. Tests are carried out to a pre-determined number of cycles unless the wire fractures prior to reaching that number of cycles. In addition to being used directly to determine the fatigue

properties of wires that are components in medical devices (e.g., braided stent or septal occluder), rotary bend wire fatigue testing is sometimes used as a surrogate to determine fatigue properties for devices not made of wires, such as endovascular stents (Ref 11). A new standard, ASTM E2948-14 Standard Test Method for Conducting Rotating Bending Fatigue Tests of Solid Round Fine Wire, was recently published and further illustrates the popularity of this test (Ref 12).

Although rotary bend wire fatigue is a relatively common test, the speed used to perform testing can vary greatly. Given that in vivo loading occurs at a much slower rate than the maximum speed of motors used in wire fatigue testers (e.g., approximately 72 beats per minute for cardiac loading versus 25,000 or more revolutions per minute (RPM) for a high-speed motor), it is necessary to understand how quickly tests can be conducted so that results can be obtained in a reasonable timeframe and still be used to establish fatigue safety at slower in vivo loading rates. One recent study compared two different rotary bend wire fatigue test methods at different test speeds (500, 1000, and 5000 RPM) using nitinol wire (Ref 13). The study found that both test methods (guided and unguided) resulted in a similar number of cycles to fracture at the test speeds employed in the study. A previous study conducted in our laboratory used the unguided rotary bend fatigue test method to determine the fatigue life of nitinol wire at speeds of 36, 360, and 3600 RPM (Ref 14). In this study, the fatigue life was found to increase with test speed at certain alternating strain levels. Tobushi et al. investigated the effect of test speed (100, 300, 500, and 1000 RPM) on nitinol fatigue in an unguided wire fatigue setup in water and found no significant difference in fatigue life for the speeds and strain amplitudes tested (Ref 15). In the same study, Tobushi et al. found that fatigue life tended to decrease with increased test speed when tests were conducted in air, but they attributed this difference to

**Jason D. Weaver**, Division of Applied Mechanics, Center for Devices and Radiological Health - Office of Science and Engineering Laboratories, United States Food & Drug Administration, Silver Spring, MD; and **Erick J. Gutierrez**, Division of Applied Mechanics, Center for Devices and Radiological Health - Office of Science and Engineering Laboratories, United States Food & Drug Administration, Silver Spring, MD and Oak Ridge Institute for Science and Education, Oak Ridge, TN. Contact e-mail: jason.weaver@fda.hhs.gov.

a larger temperature increase in the wires tested at the faster test speeds in air; tests conducted in water exhibited no temperature change as test speed was increased. Wire fatigue studies of medical alloys other than nitinol are not as common and to the authors' knowledge have not systematically investigated the effects of test speed or test method (Ref 4, 16-18).

Because data from wire fatigue testing are used to calculate fatigue safety factors during medical device design, it is essential that the fatigue data are reliable so that the safety factor predictions are also reliable. Therefore, in this study we have chosen to evaluate three different wire fatigue test methods at speeds ranging from approximately physiologic to near the maximum capabilities of motors typically used in rotary bend wire fatigue testers to determine how these two important factors affect the number of cycles to fracture in three common medical device alloys. Additionally, because strain rate sensitivity was suspected to be affecting fatigue results, one of the three alloys was selected for supplemental uniaxial tension tests at varying strain rates to determine whether strain rate sensitivity could be affecting the fatigue results.

The mention of commercial products, their sources, or their use in connection with materials reported herein is not to be

construed as either an actual or implied endorsement of such products by the Department of Health and Human Services.

## 2. Methods

### 2.1 Rotary Bend Wire Fatigue

Fatigue tests were conducted using Blockwise Engineering Model FTXH wire fatigue testers (Tempe, AZ) with one of three test setups as shown in Fig. 1:

- Unguided
- Guided Disc
- Guided Block

The fixtures for the Guided Disc and Guided Block were custom-made polyoxymethylene parts that attached to the wire fatigue testers so that the same motors and chucks were used in all three test setups. The three different test setups are intended to be inclusive of multiple published methods of conducting wire fatigue testing. Tests were conducted at speeds ranging

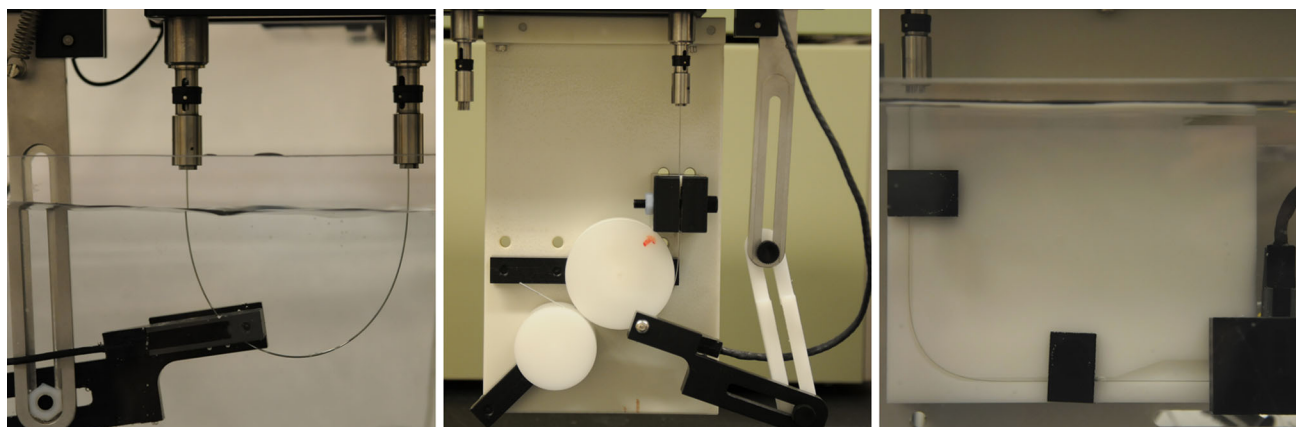


**Fig. 1** Wire fatigue test methods, from left to right: Unguided, Guided Disc, and Guided Block. Wires in the unguided test are driven by chucks at both ends. Wires in the Guided Disc setup are driven at one end, passed through a bushing, wrapped around a grooved disc with a specified radius of curvature, held in place with a pusher grooved disc, and then are free at the other end of the wire. Wires in the Guided Block setup are driven on one end and free on the other; the majority of the wire is maintained within a groove in the block that is machined to include a specified radius of curvature

**Table 1** Number of cycles to fracture for fatigue testing grouped by test method, speed, and material presented as mean  $\pm$  standard deviation

Material and alternating strain	Test method	Test speed, RPM					
		100	500	1000	5000	10,000	35,000
Nitinol, 1.0%	Unguided	5866 $\pm$ 644	7174 $\pm$ 62	7419 $\pm$ 115	8579 $\pm$ 764	10,292 $\pm$ 379	10,679 $\pm$ 663
	Guided Disc	5483 $\pm$ 527	6204 $\pm$ 328	6457 $\pm$ 155	8526 $\pm$ 531	9178 $\pm$ 388	11,287 $\pm$ 585
	Guided Block	5759 $\pm$ 351	6159 $\pm$ 579	6791 $\pm$ 297	8792 $\pm$ 441	9279 $\pm$ 279	12,154 $\pm$ 680
Stainless steel, 0.5%	Unguided	17,725 $\pm$ 820	19,884 $\pm$ 1638	22,716 $\pm$ 2752	29,801 $\pm$ 670	45,840 $\pm$ 6265	61,328 $\pm$ 3006
	Guided Disc	17,805 $\pm$ 522	22,114 $\pm$ 1690	26,051 $\pm$ 1209	40,429 $\pm$ 1967	45,163 $\pm$ 9017	57,481 $\pm$ 7559
	Guided Block	17,552 $\pm$ 813	20,212 $\pm$ 2172	24,854 $\pm$ 372	41,790 $\pm$ 3540	33,583 $\pm$ 10,154	49,695 $\pm$ 7157
Cobalt chromium, 0.5%	Unguided	23,205 $\pm$ 1717	41,129 $\pm$ 4123	48,999 $\pm$ 8322	83,108 $\pm$ 5385	86,821 $\pm$ 5390	141,929 $\pm$ 10,907
	Guided Disc	23,360 $\pm$ 2419	41,831 $\pm$ 6463	46,344 $\pm$ 5407	89,051 $\pm$ 2670	116,972 $\pm$ 13,225	116,806 $\pm$ 2389
	Guided Block	29,014 $\pm$ 6839	37,876 $\pm$ 10,670	47,854 $\pm$ 6741	73,138 $\pm$ 2588	96,002 $\pm$ 19,386	128,587 $\pm$ 16,360

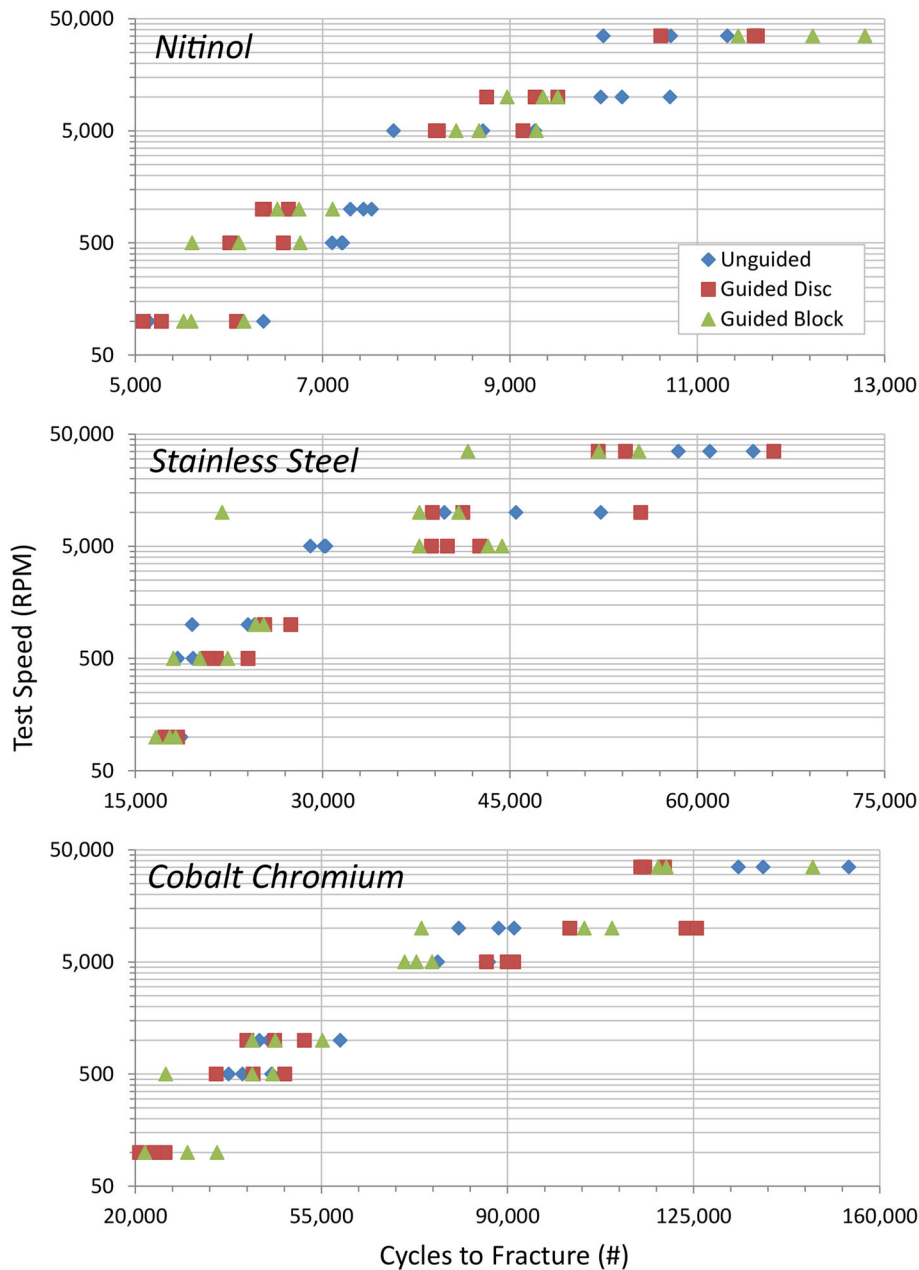


**Fig. 2** Test speed vs. number of cycles to fracture for each material

from 100 to 35,000 RPM. The alternating strain,  $\epsilon_a$ , in the wire was determined by

$$\epsilon_a = \frac{d}{2R} \times 100\%, \quad (\text{Eq 1})$$

where  $d$  is the wire diameter and  $R$  is the radius of curvature. For the unguided test setup, the minimum radius of curvature occurs at the apex and is based on a relationship between the distance between the two motors and the wire length that has been described previously (Ref 14). The radii of curvature for the Guided Disc and Guided Block setups were determined by the radius machined into the polyoxymethylene material. All fatigue tests were conducted in deionized water at 37 °C.

Three common medical device alloys were selected and each one was tested at a particular alternating strain value in

each of the three test setups. Three samples of each alloy were tested at every test speed and test setup. The alloys were

- Electropolished nitinol (ASTM F2063) at 1.0% alternating strain
- Stainless steel alloy (ASTM F138) at 0.5% alternating strain
- Cobalt chromium alloy (ASTM F1058) at 0.5% alternating strain

Nitinol wire was obtained from Motion Dynamics Corporation (Fruitport, MI). Stainless steel and cobalt chromium alloy wires were obtained from Fort Wayne Metals (Fort Wayne, IN). The nitinol wire was in an annealed condition; the stainless steel and cobalt chromium alloys had been subjected to 75 and

60% cold work, respectively. Nitinol wire was 0.500 mm in diameter while the stainless steel and cobalt chromium alloy wires were 0.178 mm in diameter. After fatigue testing, the fracture surfaces of several specimens from tests at different speeds were examined with scanning electron microscopy (SEM) using a JEOL JSM-3690LV (Tokyo, Japan).

## 2.2 Uniaxial Tension

Uniaxial tension tests were conducted with an Instron E3000 tester (Norwood, MA) with a 1 kN load cell using pneumatic grips to hold specimens in place during testing. Tests were conducted on 0.500 mm diameter stainless steel wire with 75% cold work that was supplied by Fort Wayne Metals (Fort Wayne, IN). Specimens were pulled at constant crosshead speed and strain was measured using a video extensometer system. The initial distance between grips was approximately 70 mm and the initial distance between the two video extensometer markers was approximately 20 mm. Strain rates varied from  $1.7 \times 10^{-6}$  to  $1.7 \times 10^{-2} \text{ s}^{-1}$  and all tests were conducted in air at room temperature. Between five and nine specimens were tested at each of the five strain rates.

## 2.3 Statistical Analysis

Linear regression analyses were performed on fatigue test data to determine if there was a statistically significant relationship between the number of cycles to fracture and test

speed for each material. An analysis of covariance was performed using test speed as a covariate to determine whether the test setup had a statistically significant effect on number of cycles to fracture for each material. Linear regression analyses were also performed on the uniaxial tensile test data to determine if there was a significant effect of strain rate on individual mechanical parameters (yield strength, Young's modulus, ultimate strength, and strain at break). Because strain rate varied on a logarithmic scale during testing and we used a linear regression statistical analysis, we took the natural logarithm of strain rate and used those values instead of the raw strain rate values for statistical analyses. All statistical analyses were conducted with Minitab software (Minitab Inc., State College, PA).

## 3. Results

### 3.1 Rotary Bend Wire Fatigue

In terms of test speed, a noticeable increase in number of cycles to fracture was seen as the test speed was increased for all three alloys tested. Linear regression analysis revealed statistically significant relationships between number of cycles to fracture and test speed for nitinol ( $R^2 = 0.737$  and  $P < 0.001$ ), stainless steel ( $R^2 = 0.714$  and  $P < 0.001$ ), and cobalt chromium ( $R^2 = 0.713$  and  $P < 0.001$ ). As test speed was increased from 100 to 35,000 RPM, the average number of

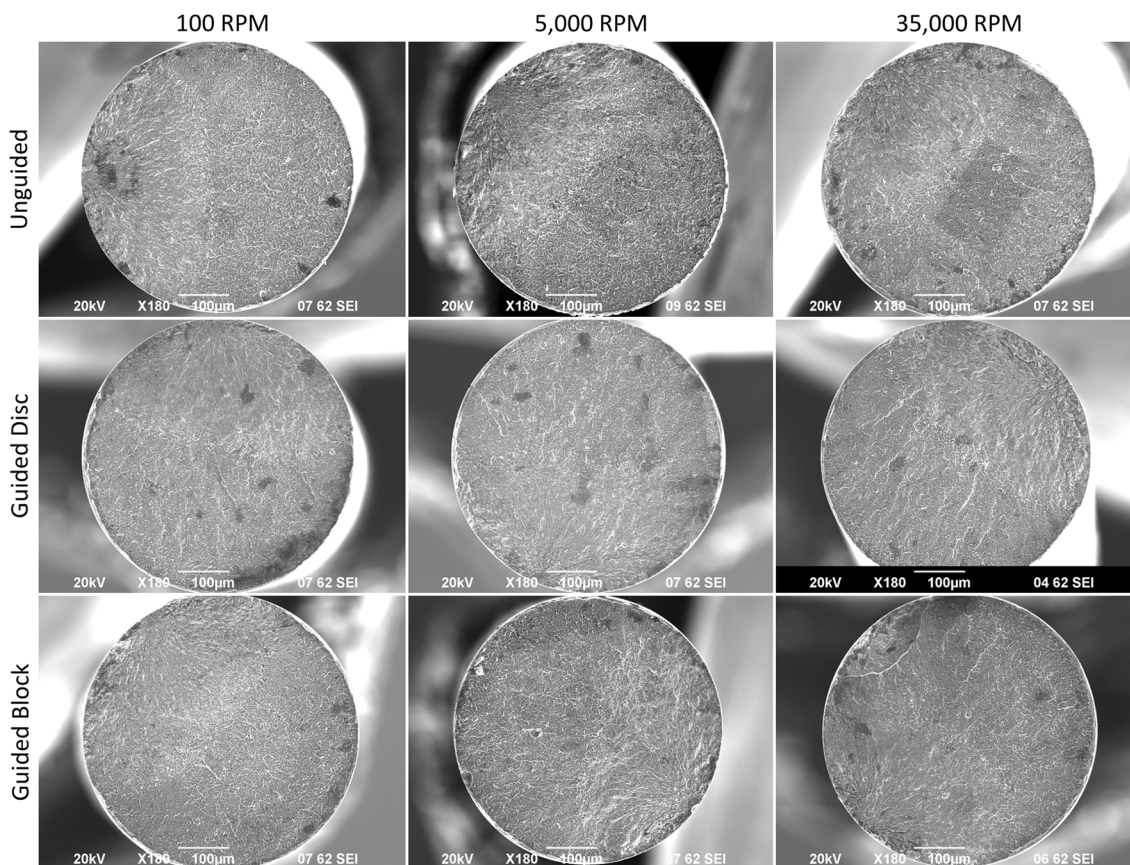
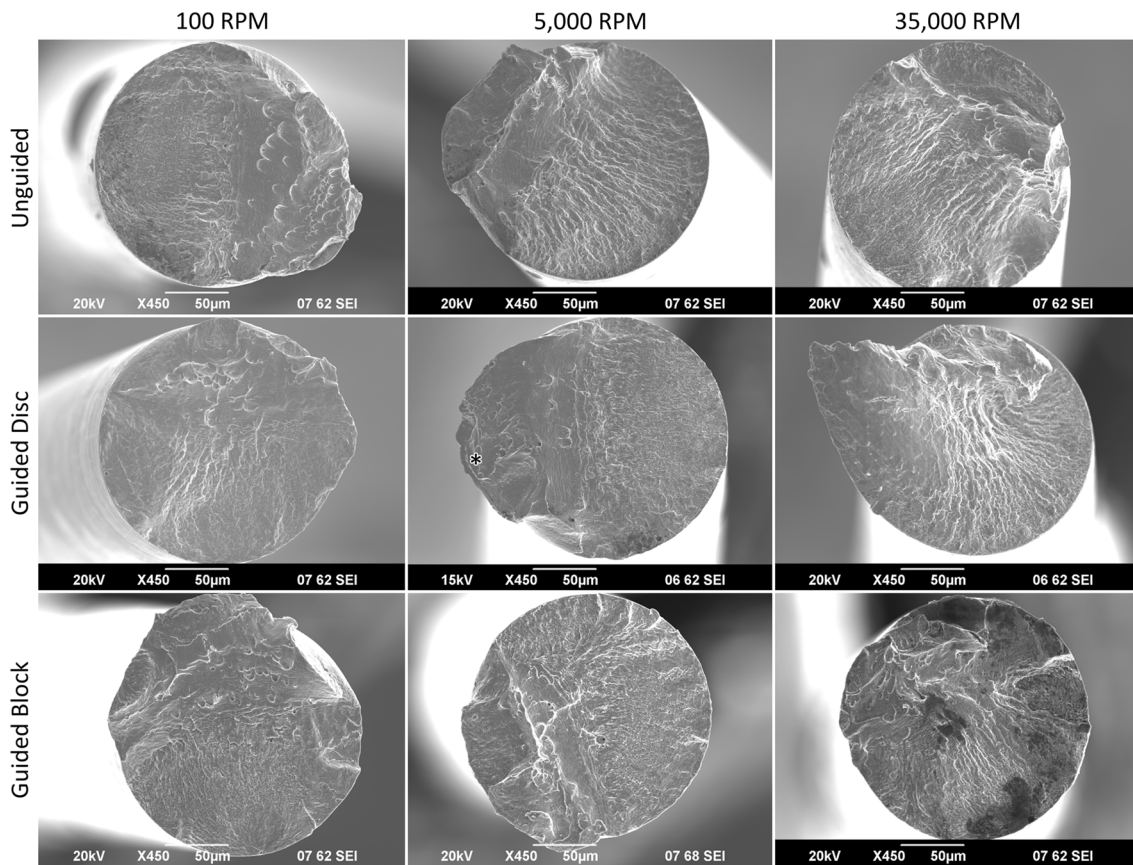


Fig. 3 SEM images of nitinol wire fracture surfaces for varying test methods and speeds



**Fig. 4** SEM images of stainless steel wire fracture surfaces for varying test methods and speeds. The \* highlights one of the twisted/smearing regions for illustrative purposes

cycles until fracture increased by 2.0-fold for nitinol, 3.2-fold for stainless steel, and 5.1-fold for cobalt chromium; the average number of cycles to fracture for all specimens tested can be found in Table 1. As can be seen by the overlapping data points for each test method in the plots at each individual test speed in Fig. 2, the different fatigue test methods resulted in a similar number of cycles to fracture. The cobalt chromium alloy, for example, has Guided Block data points that fall toward the minimum, intermediate, and maximum values as the results of each test speed are individually examined. Furthermore, analysis of covariance revealed no statistical difference in number of cycles to fracture among the test setups for nitinol ( $P = 0.401$ ), stainless steel ( $P = 0.405$ ), or cobalt chromium ( $P = 0.872$ ).

SEM images of fracture surfaces of each material are presented in Fig. 3, 4, and 5. Representative images from the minimum (100 RPM), an intermediate (5000 RPM), and the maximum (35,000 RPM) test speed are shown for each fatigue test method. All the images show characteristic fatigue failure regions of crack growth and fast fracture. Overall, for each material all the images are qualitatively similar in terms of the size of the fatigue crack and in terms of the features in each region. No large differences could be found among the different fatigue test methods or test speeds although some stainless steel and cobalt chromium wires tested with the Guided Disc and Guided Block methods (e.g., 5000 RPM Guided Disc in Fig. 4 and 100 RPM Guided Block in Fig. 5) did have features in the fast fracture region that appeared twisted and/or smeared.

### 3.2 Uniaxial Tension

Results of tensile experiments on the stainless steel alloy are presented in Table 2. Linear regression analyses found that strain at break ( $R^2 = 0.001$  and  $P = 0.854$ ) and yield strength ( $R^2 = 0.097$  and  $P = 0.078$ ) were fairly insensitive to changes in the natural logarithm of strain rate. However, Young's modulus ( $R^2 = 0.289$  and  $P = 0.001$ ) and, in particular, ultimate strength ( $R^2 = 0.969$  and  $P < 0.001$ ) did have statistically significant relationships with both parameters increasing with increasing strain rate. Representative stress-strain curves for the different strain rates can be seen in Fig. 6. It should be noted that in Fig. 6 the stress value at 0% strain is slightly greater than 0 MPa. This is because a small pre-load of 3.0 N was applied prior to initiating the test in order to remove any grip slack. Generally, the stress-strain curve shifted upwards as the strain rate was increased.

## 4. Discussion

As can be seen in Table 1 and Fig. 2, 3, 4, and 5, the three rotary bend wire fatigue methods tested here produced similar fatigue results. Moreover, an analysis of covariance utilizing test speed as a covariate found no statistically significant difference in number of cycles to fracture among test setups for all three alloys. This finding supports recent work by Norwich that compared an unguided and guided block type of test at a

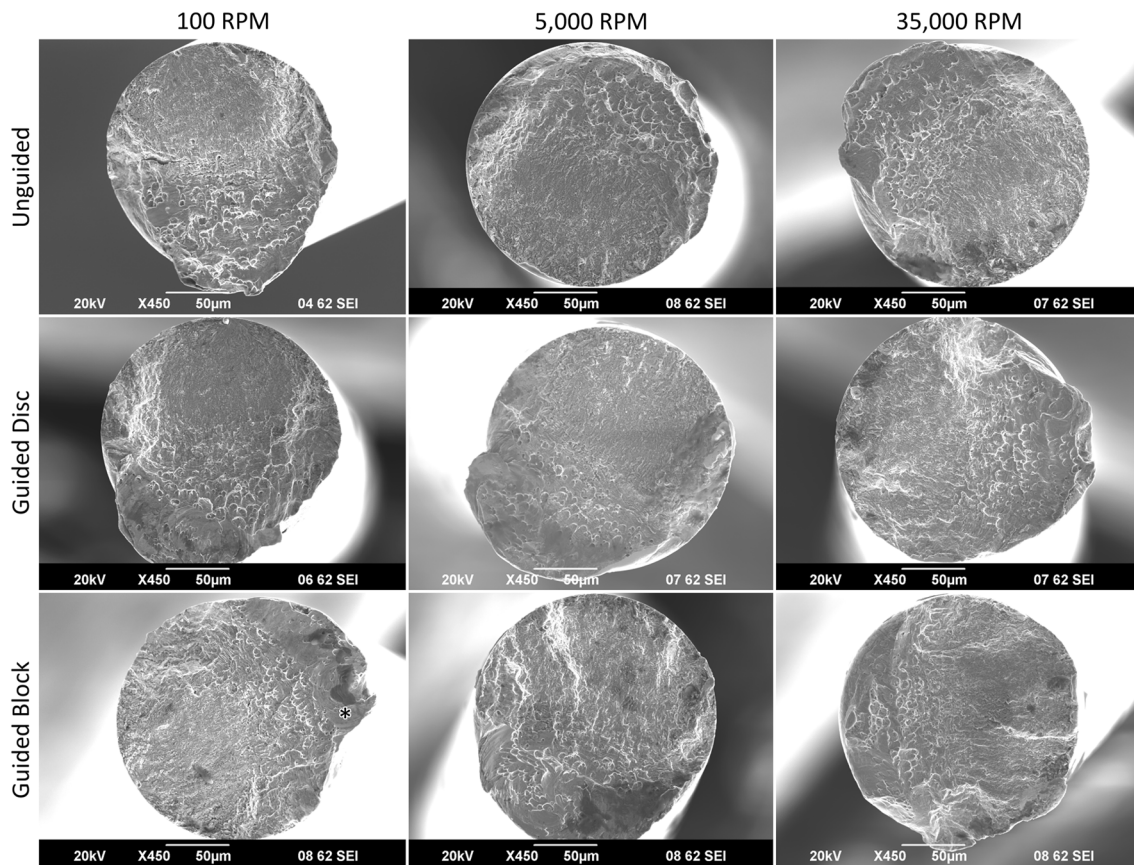


**Fig. 5** SEM images of cobalt chromium wire fracture surfaces for varying test methods and speeds. The \* highlights one of the twisted/smeared regions for illustrative purposes

**Table 2** Results of uniaxial tensile testing of stainless steel wire for each strain rate presented as mean  $\pm$  standard deviation

Strain rate, $s^{-1}$	Yield strength, MPa	Young's modulus, GPa	Ultimate strength, MPa	Strain at break, %
$1.7 \times 10^{-6}$	$1029 \pm 19$	$123 \pm 8$	$1341 \pm 3$	$3.5 \pm 0.2$
$1.7 \times 10^{-5}$	$1037 \pm 16$	$124 \pm 4$	$1352 \pm 3$	$3.6 \pm 0.4$
$1.7 \times 10^{-4}$	$1044 \pm 46$	$133 \pm 9$	$1365 \pm 4$	$3.7 \pm 0.4$
$1.7 \times 10^{-3}$	$1032 \pm 66$	$138 \pm 18$	$1381 \pm 3$	$3.8 \pm 0.6$
$1.7 \times 10^{-2}$	$1076 \pm 46$	$141 \pm 17$	$1404 \pm 1$	$3.4 \pm 0.2$

smaller range of test speeds (Ref 13). Previous work in our laboratory (Ref 14) had suggested that small vibrations during unguided fatigue testing might affect fatigue life results and that guided tests might provide more consistent results since the guides could reduce vibrations. However, based on the present results and those of Norwich (Ref 13), it appears that the small vibrations which can be seen during unguided wire fatigue testing do not greatly affect the fatigue life results and that unguided and guided test methods produce similar results. One potential source of differences between unguided and guided tests is that guided tests constrain the wire in such a way that the entire length of wire undergoing alternating strain is at the same radius of curvature whereas the wire in an unguided test has a radius of curvature that changes along its length resulting in strain values that are zero at the chucks and reach a maximum at the apex. This difference could potentially lead to differing results and difficulties interpreting results since

unguided wires can fracture at locations away from the maximum strain. When fracture occurs away from the apex in an unguided test, it is possible to determine the strain at the fracture location by using a correction factor as described in ASTM E2948-14 (Ref 12). In our tests, nearly all of the unguided test specimens fractured close to the apex resulting in strains at the fracture location of at least 95% of the maximum strain value with the exception of two cobalt chromium wires. This suggests that the difference in radius of curvature between test methods had little effect on our fatigue life results. Additionally, although the results were not presented, correction factors for the unguided tests did not vary with test speed.

In Fig. 4 and 5, some of the stainless steel and cobalt chromium wires (e.g., 5,000 RPM Guided Disc in Fig. 4 and 100 RPM Guided Block in Fig. 5) contained features in the fast fracture region that appear to be twisted or smeared. These twisted and smeared features were not observed in the nitinol

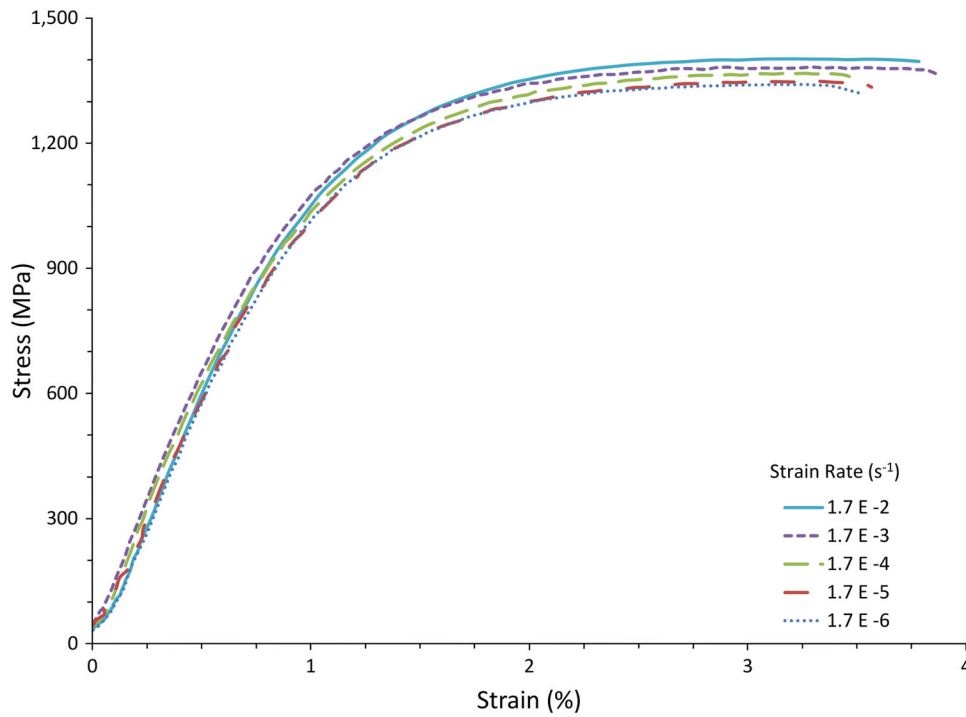


**Fig. 6** Representative stress-strain plots of stainless steel wire in uniaxial tension at varying strain rates. Prior to testing, all specimens were subjected to a small pre-load of 3.0 N in order to remove slack in the grips

**Table 3** Constants for relationship between fatigue life and test speed

Material and alternating strain	$\alpha$	$\beta$	$R^2$
Nitinol, 1%	3117	0.121	0.906
Stainless steel, 0.5%	6332	0.204	0.870
Cobalt chromium, 0.5%	6630	0.289	0.937

wires or in any of the unguided wire tests. These features, while not present in all imaged samples, could be related to how the wires were constrained during testing. In the unguided test method, both ends of the wire were driven whereas in the two guided test methods, only one end of the wire was driven while the other end was free. This difference in wire end constraints could have led to some wires in the guided tests rotating for several cycles during the fast fracture process, with the driven end essentially pulling along the free end of the wire. During this process, the two fracture surfaces might have rubbed against each other as the last bit of material was twisted until the fracture was complete. Wires tested by the unguided method, on the other hand, being driven on both ends, may have fractured more quickly after the fatigue crack had grown to a critical size. The nitinol wire fracture surfaces did not exhibit these features and looked more consistent across test methods. It is unclear what may be the underlying cause of these differences between the nitinol and the other two alloys, though we suspect it could be due to a difference in elastic modulus between the materials. Nevertheless, it is important to note that although these minor qualitative differences were observed in some of the imaged fracture surfaces, there was still no discernable difference in fatigue life among the three wire fatigue test methods.

With regards to test speed, the data gathered here show that, at least for these three materials and alternating strains, the number of cycles to fracture increases with test speed. In Fig. 2, it can be seen that the cycles to fracture data points spread out more as the test speed is increased. This is similar to typical stress-life curves wherein greater variability is seen at longer fatigue lives than in shorter ones (Ref 19) and is somewhat expected given the increase in cycles to fracture seen at faster test speeds. Based on the data, a relationship between the number of cycles to fracture,  $N_f$ , and the test speed in RPM,  $\omega$ , can be written as follows

$$N_f = \alpha \omega^\beta, \quad (\text{Eq 2})$$

where  $\alpha$  and  $\beta$  are constants determined from the test data. Using Microsoft Excel (Redmond, WA), these constants in addition to the  $R^2$  coefficient of determination values were determined as seen in Table 3. The coefficients of determination are relatively high for each of the three alloys indicating that the proposed relationship in Eq 2 is a good fit for the data. Whether or not these relationships would hold for different materials, alternating strains, or test speeds is not presumed and would have to be investigated in future work. Although it is relatively uncommon to observe an increase in fatigue life as test speed increases, other researchers have observed a similar effect in some materials, though at much faster test speeds. Papakyriacou et al. found that tantalum tested at 20 kHz had increased fatigue life compared to tests conducted at 100 Hz (Ref 20). Nonaka et al. tested steel used in bullet train axles at 10 Hz, 400 Hz, and 19.8 kHz and found that tests performed at 19.8 kHz led to increased fatigue limits compared to the two slower speeds (Ref 21).

Our tensile tests of ASTM F138 stainless steel alloy wire at varying strain rates revealed strain rate sensitivity with

statistically significant increases in ultimate strength as the strain rate was increased. Other researchers have similarly shown that the materials studied here can exhibit strain rate sensitivity. In tensile experiments with nitinol wire, Tobushi et al. found that increasing strain rate led to an increase in the martensite transformation stress (Ref 22). In a study of as-drawn MP35N alloy wires (a cobalt chromium alloy similar to the one studied here), Prasad et al. found the wires to exhibit strain rate sensitivity and increased strength as the strain rate was increased (Ref 18). Although other factors could be involved, the phenomena of increased strength shown at higher strain rates in tensile testing might explain the apparent increase in the number of cycles to fracture in fatigue with increasing test speed. As the fatigue test speed is increased, the wires have increased strength leading to a slight upward shift in their fatigue strength. Although determining the precise cause of the strain rate sensitivity falls outside the scope of the present study, work by Ahadi and Sun suggest that it may be related to grain size (Ref 23).

Since a common use of rotary bend wire fatigue tests is to aid in predicting fatigue safety factors of medical devices, it is critical that the fatigue data are reliable and predictive of in vivo conditions. Because in vivo loading of medical devices typically occurs at a rate of 1 Hz or slower while fatigue testing is conducted at a much faster rate, we must consider how test speed affects results and subsequently fatigue safety factors. Based on the materials and alternating strains tested in this study, wire fatigue data collected at an accelerated test rate could lead to an over prediction of fatigue life when the same wire is loaded at a slower, in vivo rate. However, our data set is not comprehensive and we should not assume that all materials would exhibit this behavior. Future work should examine how test speed affects fatigue life over a much greater range of alternating strains. Additionally, our experiments were conducted in deionized water which is not representative of the corrosive in vivo environment. It remains to be seen to what extent an environment like PBS would affect the fatigue life of medical device alloys at different test speeds. Overall, much work remains to be done to ensure that laboratory fatigue testing done at accelerated rates is representative of in vivo loading conditions so that we can more accurately predict fatigue safety of medical devices.

## 5. Conclusions

The principal conclusions from the study are as follows:

- The rotary bend wire fatigue test methods studied here do not have an appreciable effect on the fatigue life of the materials studied.
- Fatigue life increased with increasing test speed for all three wire fatigue test methods. This increase appears to be due to strain rate sensitivity in the materials selected for this study.

## Acknowledgments

This project was supported by the Division of Applied Mechanics, FDA's Medical Countermeasures Initiative, and an appointment to the Research Participation Program at the Center

for Devices and Radiological Health administered by the Oak Ridge Institute for Science and Education through an interagency agreement between the U.S. Department of Energy and the U.S. Food and Drug Administration. The authors would like to thank the following individuals for their thoughtful insights at various stages of this project: Matthew Di Prima, Shiril Sivan, Terry Woods, Kenneth L. Jerina, M. R. Mitchell, and L. D. Timmie Topoleski.

## References

1. M. Lenz, S.M. Perren, R.G. Richards, T. Muckley, G.O. Hofmann, B. Gueorguiev, and M. Windolf, Biomechanical Performance of Different Cable and Wire Cerclage Configurations, *Int. Orthop.*, 2013, **37**, p 125–130
2. T. Peitsch, A. Klocke, B. Kahl-Nieke, O. Prymak, and M. Epple, The Release of Nickel from Orthodontic NiTi Wires is Increased by Dynamic Mechanical Loading but not Constrained by Surface Nitridation, *J. Biomed. Mater. Res. A*, 2007, **82A**, p 731–739
3. E. Henderson, D.H. Nash, and W.M. Dempster, On the Experimental Testing of Fine Nitinol Wires for Medical Devices, *J. Mech. Behav. Biomed. Mater.*, 2011, **4**, p 261–268
4. P.A. Altman, J.M. Meagher, D.W. Walsh, and D.A. Hoffmann, Rotary Bending Fatigue of Coils and Wires Used in Cardiac Lead Design, *J. Biomed. Mater. Res.*, 1998, **43**, p 21–37
5. W. Sun, A. Abad, and M.S. Sacks, Simulated Bioprosthetic Heart Valve Deformation Under Quasi-static Loading, *J. Biomech. Eng.*, 2005, **127**, p 905–914
6. D.W. Norwich and A. Fasching, A Study of the Effect of Diameter on the Fatigue Properties of NiTi Wire, *J. Mater. Eng. Perform.*, 2009, **18**, p 558–562
7. A.R. Pelton, J. Fino-Decker, L. Vien, C. Bonsignore, P. Saffari, M. Launey, and M.R. Mitchell, Rotary-Bending Fatigue Characteristics of Medical-Grade Nitinol Wire, *J. Mech. Behav. Biomed. Mater.*, 2013, **27**, p 19–32
8. M. Rahim, J. Frenzel, M. Frotscher, J. Pfetzing-Micklisch, R. Steegmuller, M. Wohlschlogel, H. Mughrabi, and G. Eggeler, Impurity Levels and Fatigue Lives of Pseudoelastic NiTi Shape Memory Alloys, *Acta Mater.*, 2013, **61**, p 3667–3686
9. M. Wagner, T. Sawaguchi, G. Kaustrater, D. Hoffken, and G. Eggeler, Structural Fatigue of Pseudoelastic NiTi Shape Memory Wires, *Mater. Sci. Eng. A*, 2004, **378**, p 105–109
10. S. Gupta, A.R. Pelton, J.D. Weaver, X.Y. Gong, and S. Nagaraja, High Compressive Pre-strains Reduce the Bending Fatigue Life of Nitinol Wire, *J. Mech. Behav. Biomed. Mater.*, 2015, **44**, p 96–108
11. R.V. Marrey, R. Burgermeister, R.B. Grishaber, and R.O. Ritchie, Fatigue and Life Prediction for Cobalt-Chromium Stents: A Fracture Mechanics Analysis, *Biomaterials*, 2006, **27**, p 1988–2000
12. ASTM E2948-14, *Standard Test Method for Conducting Rotating Bending Fatigue Tests of Solid Round Fine Wire*, ASTM International, West Conshohocken, PA, 2014
13. D.W. Norwich, A Comparison of Zero Mean Strain Rotating Beam Fatigue Test Methods for Nitinol Wire, *J. Mater. Eng. Perform.*, 2014, **23**, p 2515–2522
14. J.D. Weaver, S. Gupta, and T.O. Woods, The Effects of Test Speed on Fatigue Life of Nitinol Wire in Rotary Bend. *Fatigue and Fracture of Medical Metallic Materials and Devices STP 1559*, M.R. Mitchell, S.W. Smith, T. Woods, and B.T. Berg, Eds., ASTM International, West Conshohocken, PA, 2013, p 1–17, doi:10.1520/STP155920120213, 2013
15. H. Tobushi, T. Hachisuka, S. Yamada, and P.H. Lin, Rotating-Bending Fatigue of a TiNi Shape-Memory Alloy Wire, *Mech. Mater.*, 1997, **26**, p 35–42
16. C. Clerc, M. Jedwab, D. Mayer, P. Thompson, and J. Stinson, Assessment of Wrought ASTM F1058 Cobalt Alloy Properties for Permanent Surgical Implants, *J. Biomed. Mater. Res.*, 1997, **38**, p 229–234
17. A. Scheiner, J. Mortimer, and T. Kicher, A Study of the Fatigue Properties of Small Diameter Wires Used in Intramuscular Electrodes, *J. Biomed. Mater. Res.*, 1991, **25**, p 589–608



18. M. Prasad, M.W. Reiterer, and K.S. Kumar, Microstructure and Mechanical Behavior of an As-Drawn MP35 N Alloy Wire, *Mater. Sci. Eng. A*, 2014, **610**, p 326–337
19. R.I. Stephens, A. Fatemi, R.R. Stephens, and H.O. Fuchs, *Metal Fatigue in Engineering*, 2nd ed., Wiley, New York, 2001
20. M. Papakyriacou, H. Mayer, C. Pypen, H. Plenk, and S. Stanzl-Tschegg, Influence of Loading Frequency on High Cycle Fatigue Properties of b.c.c. and h.c.p. Metals, *Mater. Sci. Eng. A*, 2001, **308**, p 143–152
21. I. Nonaka, S. Setowaki, and Y. Ichikawa, Effect of Load Frequency on High Cycle Fatigue Strength of Bullet Train Axle Steel, *Int. J. Fatigue*, 2014, **60**, p 43–47
22. H. Tobushi, Y. Shimeno, T. Hachisuka, and K. Tanaka, Influence of Strain Rate on Superelastic Properties of TiNi Shape Memory Alloy, *Mech. Mater.*, 1998, **30**, p 141–150
23. A. Ahadi and Q.P. Sun, Effects of Grain Size on the Rate-Dependent Thermomechanical Responses of Nanostructured Superelastic NiTi, *Acta Mater.*, 2014, **76**, p 186–197